An Analysis of Crack Propagation Paths at Implant/Bone-Cement Interfaces

B. A. O. McCormack
Bioengineering Research Centre,
Department of Mechanical Engineering,
University College Dublin, Belfield,
Dublin 4, Ireland

P. J. Prendergast
Department of Mechanical Engineering,
Trinity College,
Dublin 2, Ireland

Clinical follow-up studies of joint replacements indicate that debonding of the implant from the bone-cement is the first mechanical event of loosening. Debonding can occur due to unsustainable interface stresses, usually initiated from defects along the interface. Such defects, or flaws, are inevitably introduced during the surgical procedure and from polymerisation shrinkage. Debonding leads to increased stresses within the cement mantle. This study is concerned with modelling the propagation of a crack from the debonded region on the cement/implant interface under physiological loading conditions for different implant materials and prosthesis designs. Using the theory of linear fracture mechanics for bimaterial interfaces, the behaviour of a crack along an interface between implant materials, under various states of stress, is studied. Specifically, a model is developed to determine the conditions under which a debonded region, along an otherwise bonded interface, will either propagate along the interface or will "kink" into the cement mantle. The relationship between the stress state and the crack propagation direction at the interface is then predicted for different interface materials, and it is shown that different crack directions exist for different materials, even when the stress state is the same. Furthermore, the crack behavior is shown to be dependent on the ratio of normal stress to shear stress at the interface and this may be important for the design optimisation of load-bearing cemented prostheses. Finally, the likelihood that an interface crack will propagate into the cement mantle is explored using a suitable fracture criterion.

Introduction

It is well accepted that cracks exist in the cement mantle and at the cement/implant interface. These cracks arise typically from flaws such as pores in the mantle or on the cement/implant interface (James et al., 1993), or from failure of the interface bond due to stress overload (Huiskes, 1993). Jasty et al. (1991) studied the failure of 11 implanted femurs retrieved at autopsy whose service life ranged from two weeks to seventeen years. Even though there was no radiographic evidence of loosening, there was evidence of cement/implant debonding located typically at the proximal anterior and the distal anterior surfaces. All cement mantles were cracked to some degree after three years of service life, and those with ten years or more service life had cracks completely through the cement mantles. They concluded that the cement/implant interface failures occur first, and that these cracks proceed into the cement mantle either radially or circumferentially (Maloney et al., 1989).

Variations in the techniques used for preparing and inserting the bone cement are considered to influence the service life of an implant (Harris, 1994). Significant porosity (15–28 percent) has been observed at the cement/implant interface in cement mantles removed at revision, for a variety of implant designs (James et al., 1993), and in mantles which had originally been implanted using improved cementing techniques (Helmke et al., 1992). This would indicate that improved cementing techniques are not enough to ensure a defect-free cement/implant interface.

In primary cemented total hip arthroplasties, it is generally seen that mechanical loosening begins by either (i) failure of the cement/implant bond (Huiskes, 1993), or (ii) fracture of the cement mantle directly from defects such as air bubbles (Culleton et al., 1993). In the case of (i), cement/implant interface failure may lead to higher stresses generally within the mantle (Huiskes, 1985; Verdonschot, 1995); this may activate other crack sites at the cement/stem interface and within the cement mantle, such as those introduced from polymerisation shrinkage or mixing technique (Krause and Mathis, 1988). Eventually multi-site fracture occurs, leading to disintegration of the cement interlock.

It is well acknowledged that *both* mechanical and biological processes contribute to failure of an arthroplasty, however the mechanical process is considered to be the dominant failure process at the early stages of the service life. This, together with the observations made from autopsy specimens, leads to the conclusion that cracks must play a determining role in the failure process. Indeed, clinically, the presence of interface lucency (i.e., an interface crack or debond) can be interpreted as a sign of impending loosening, or that loosening has already occurred and is one of the indications for revision surgery (Harris, 1994). Therefore, in order to better understand the role of cracks in the failure process, it would be useful to model crack behaviour in the implant structure, and in particular the behaviour of pre-existing cracks at cement/implant interfaces under physiological loading.

Experimentally and theoretically, high stresses have been shown to exist proximally at the hip prosthesis/cement interface and in particular at the interface on the medial aspect in the proximal region (Raab et al., 1981; Verdonschot and Huiskes, 1992). Maximal cement stresses at the distal tip of the stem have also been predicted (Lewis et al., 1984). These observations depend on the type of model and loading conditions applied in the model but never-the-less indicate the regions most likely to experience high stresses. Using finite element models, Harrigan et al. (1992) concluded that the most likely failure sites were: (*a*) for one leg stance; at the cement/implant interface near the tip on the medial aspect, and in the cement bulk below the distal tip of the prosthesis; and (*b*) for stair climbing;

Contributed by the Bioengineering Division for publication in the JOURNAL OF BIOMECHANICAL ENGINEERING. Manuscript received by the Bioengineering Division September 1, 1994; revised manuscript received September 13, 1995. Associate Technical Editor: W. M. Lai.

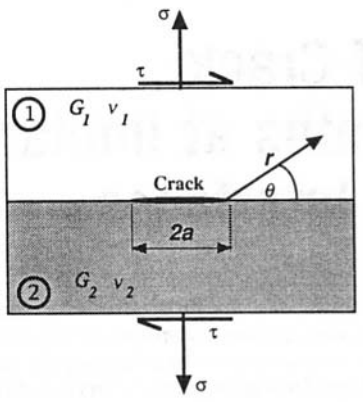

Fig. 1 Crack at a bimaterial interface. The interface between material 1 and material 2 is perfectly bonded and smooth. The angle θ is the angle at which the crack propagates or "kinks" into one of the adjacent materials. The normal and shear stresses, denoted σ and τ respectively, are the nominal interface stresses.

at the cement/implant interface on the medial aspect in the proximal region and in the cement bulk at the distal tip of the prosthesis. Dalstra (1993), in a 3D finite element analysis of cemented acetabular components, identified that for a stiff cup the cement/implant interface at the periphery of the cup is highly stressed, and that metal backing increases stresses at the interface. In this paper, these studies are used as a source of quantitative stress data on interface stresses to predict the behaviour of a crack at the cement/implant interface.

Fracture mechanics models of cracks at interfaces between any two materials of differing mechanical properties (referred to here as bimaterial interfaces) is still developing (Rice, 1988). There has been some work carried-out on applying fracture mechanics theories, in a general sense, to implant structures (Clech et al., 1985; Gharpuray et al., 1991). In this article we focus on one of the crack patterns observed clinically, i.e., a crack propagating from the prosthesis/cement interface into the bulk of the cement (Jasty et al., 1991). A linear fracture mechanics model is used to predict interface crack propagation into the cement layer as a function of the properties of the interface materials and the combination of interface stresses. The relationships derived between crack propagation direction, interface stresses, and the properties of the interface materials are considered in the context of the service life of the implant and of design features such as material selection and surface finish.

Method

An outline of bimaterial fracture mechanics as it applies to the problem introduced above will now be presented. Consider a crack of length $2a$ along a smooth interface between two different materials perfectly bonded, as shown in figure 1. Both materials are isotropic, elastic, and homogeneous. The elastic properties of the materials can be combined in one term called the bimaterial constant (denoted ϵ) which is a function of shear modulus, G, and Poisson's ratio, ν of both materials, as follows:

$$\epsilon = \frac{1}{2\pi} \ln \left\{ \left(\frac{\kappa_1}{G_1} + \frac{1}{G_2} \right) \Big/ \left(\frac{\kappa_2}{G_2} + \frac{1}{G_1} \right) \right\}, \qquad (1)$$

where

$\kappa_j = 3 - 4\nu_j$ for plane strain;
$\kappa_j = (3 - \nu_j)/(1 + \nu_j)$ for plane stress;
$j = 1$ for cement, and 2 for prosthesis;
$G = E/\{2(1 + \nu)\}$

For the two-dimensional plane strain case, the stress field near the crack tip can be represented in polar co-ordinates as shown in Fig. 1. A likely path for an interface crack is along the interface because, in general, the bonding strength of the interface is weak in comparison to the strength of the homogeneous material. However the crack may also propagate into the bone cement out of the interface (Jasty et al., 1991) and this depends on the relative strength of the interface bond and the bulk material properties local to the crack tip.

For brittle materials, such as polymethylmethacrylate (PMMA) bone-cement, it can be assumed that a crack will propagate, under monotonic loading, in the direction normal to the maximum principal stress—i.e., at an angle where the stress component σ_θ at the crack tip is a maximum. Therefore the kinking angle, θ, (the angle at which the crack would propagate out of the interface into the cement) which gives the maximum value of σ_θ, is found from

$$\frac{\partial \sigma_\theta}{\partial \theta} = 0. \qquad (2)$$

The resulting solution for θ_0 corresponding to the maximum σ_θ (presented by Yuuki and Xu, 1992) is obtained from:

$$\epsilon W_j \{2(\cos A) - (\cos\theta + 2\epsilon \sin\theta) \cos B\} + W_j \left[-(\sin A) + \{(\sin\theta - 2\epsilon \cos\theta) \cos B\} + \frac{1}{2} (\cos\theta + 2\epsilon \sin\theta) \sin B \right] - \frac{1}{W_j} \{(\epsilon \cos C) + \frac{3}{2} \sin C\} = 0 \qquad (3)$$

where

$$A = \tfrac{1}{2}\theta + \gamma$$

$$B = \tfrac{1}{2}\theta - \gamma$$

$$C = \tfrac{3}{2}\theta + \gamma$$

$$W_1 = \exp\{-\epsilon(\pi - \theta)\}$$

$$W_2 = \exp\{\epsilon(\pi + \theta)\}.$$

$$j = 1, 2$$

The parameter γ is given by:

$$\gamma = \tan^{-1}(K_2/K_1) \quad \text{for} \quad K_1 \geq 0. \qquad (4)$$

where $K = K_1 + iK_2$ is the complex stress intensity factor.[2]

Values for γ are calculated for Eq. (4) using the relationships of Rice and Sih (1965):

$$K_1 = a^{1/2} \left\{ \frac{\sigma(M + 2\epsilon N) + \tau(N - 2\epsilon M)}{\cosh \pi\epsilon} \right\} \qquad (5a)$$

$$K_2 = a^{1/2} \left\{ \frac{\tau(M + 2\epsilon N) - \sigma(N - 2\epsilon M)}{\cosh \pi\epsilon} \right\} \qquad (5b)$$

[2] It is not possible to define mode I and II stress intensities for the interface crack; the symbols K_1 and K_2 should therefore not be confused with K_I and K_{II}.

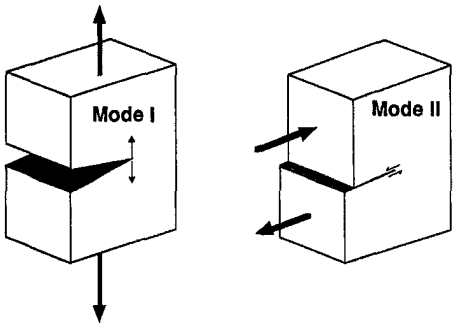

Fig. 2 Crack opening behavior under 'Mode I' and under 'Mode II' loading conditions in a homogeneous material showing remotely applied stresses and local crack tip stresses

where

$$M = \cos\left(\epsilon \log \frac{2a}{r_o}\right)$$

$$N = \sin\left(\epsilon \log \frac{2a}{r_o}\right).$$

Equations (5) are for a straight crack of length $2a$ along the interface in an infinite plane with normal and shear interface stresses, σ and τ, respectively, arising from loads applied at a large distance from the crack (Fig. 1). The $(1/r_o)$ factor has been introduced into the original equations of Rice and Sih (1965) for consistency of dimensional units. Thus, given any stress condition the components of the complex stress intensity, K_1 and K_2, at some fixed dimension, r_o, ahead of a crack (r_o = process region size, which is taken as 1/100th of the crack length, is used in this investigation) along a bimaterial interface can be calculated. Having calculated K_1 and K_2, γ is obtained from Eq. (4). Once γ is known, Eq. (3) can be solved for θ for any given interface for which the bimaterial constant ϵ is known.

It should be pointed out that, in fracture mechanics analysis of interface cracks, a theoretical difficulty arises because the stress field for an interface crack has an oscillatory singularity (Rice, 1988). Theoretically, this is interpreted as interpenetration of the two materials near the crack ends. However, this interpenetration does not occur in reality, because the crack tip region is not perfectly sharp. For the case where $|\epsilon|$ is small ($|\epsilon| < 0.1$) the effect of this oscillatory stress field on the theoretical solution is small (of the order 10^{-4}), and can be ignored in the analysis of the crack propagation under discussion.

The solution for Eq. (3) gives the angle that a crack will propagate, if indeed the crack does propagate. The ability to resist crack propagation is determined by equating the calculated crack tip stress intensity, K factor, to a material parameter, K_C, called the fracture toughness. In order to perform a fracture mechanics assessment, both K and K_C are needed; if K exceeds K_C then the crack will propagate. Whereas the stress intensity factor, K, is a calculated parameter which depends on the crack size, the applied stress and the size of the component (but is material independent), the fracture toughness is a material parameter measured experimentally and depends on the rate of loading, the temperature and the thickness of the cracked section. The fracture toughness of a material sets a maximum value for the stress intensity which can exist at a crack tip in a given material, beyond which the crack will propagate. In a homogeneous material, when a purely normal load is applied remotely to the crack tip only normal stresses arise at the tip. This is called mode I loading, and is shown in Fig. 2. Typically, the lowest value of fracture toughness occurs under Mode I loading with plane strain conditions, so it is usual to quote the fracture toughness of a material as the mode I plane strain critical stress intensity at fracture, conventionally denoted as K_{IC}. Thus, a simple fracture or failure criterion under mode I loading would be when the maximum stress intensity, call it $K_{\max}$, at the crack tip equals the K_{IC} for the material. If both shear and normal loads are applied to a crack in a homogeneous material, both shear and normal stresses exist at the crack tip. In that situation, K_I and K_{II}, the mode I and mode II stress intensities (see Fig. 2), are both used in any fracture criterion.

For the problem under consideration in this study, it would be useful to compare the stress intensities at the crack tip with a fracture toughness value to determine whether or not the crack will grow. From stress analysis we know that the defect at the cement/implant interface will experience both tensile and shear loading. And from fracture mechanics we know that, even when only a normal load is applied to a bimaterial interface containing a crack, both tensile and shear stresses exist at the crack tip (Fig. 3). In this situation, unlike the crack in a homogeneous material, an interface stress intensity cannot be uniquely defined in terms of the remotely applied normal stress alone. In addition, for a planar analysis, it is found that both components of the complex stress intensity are required to define a fracture criterion for an interface crack at a bimaterial interface subjected to a remote normal stress (Rice, 1988). A suitable fracture criterion for the mixed mode loaded crack in the model under discussion has be adopted from Yuuki and Xu (1992):

$$K_{\theta_{\max}} = f(\theta_0, \epsilon, \gamma)\frac{\sqrt{K_1^2 + K_2^2}}{2\cosh \pi\epsilon} \geq K_{IC}. \qquad (6)$$

In this case, $K_{\theta_{\max}}$ means the mode I stress intensity factor for the kinked crack of infinitesimal length in the direction θ_0. As the interface stress intensity, $K = K_1 + iK_2$, is complex the absolute value, $\sqrt{K_1^2 + K_2^2}$, is used in Eq. (6). The term $f(\theta_0, \epsilon, \gamma)$ is a defined as:

$$f = W_j\{2(\cos A) - (\cos\theta_0 + 2\epsilon \sin\theta_0)\cos B\} + \frac{1}{W_j}\cos C \quad (7)$$

where A, B, C, and W_j are defined above.

The failure criterion of Eq. (6) can be used to determine whether or not the stress condition is severe enough to cause crack propagation. The equation for $K_{\theta_{\max}}$ combines the complex stress intensities at the interface crack tip into one value, which can then be compared with the fracture toughness, K_{1C}, of the bone-cement. When $K_{\theta_{\max}}$ exceeds the critical value, K_{1C}, the crack will propagate, into the cement in the direction $\theta = \theta_0$.

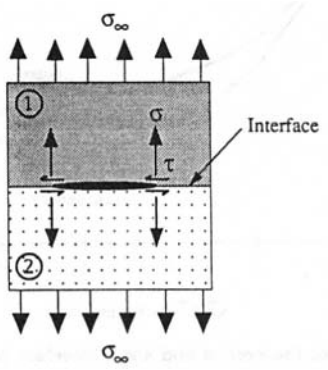

Fig. 3 Illustration showing the normal and shear stresses that arise at an interface between materials of different stiffnesses under pure normal loading

Table 1 Typical properties of materials used for orthopaedic reconstructions

Material	Young's Modulus (GPa)	Poisson's Ratio	Shear Modulus (GPa)
PMMA	4.0	0.30	1.54
Titanium	109.0	0.33	41.00
Cr/Co Alloy	241.0	0.30	92.60
Stainless Steel	200.0	0.30	77.00
Bone	0.3	0.32	0.13
UHMWPE	8.4	0.40	3.00

Table 2 Bimaterial constant, ϵ, for typical material combinations occuring in orthopaedic reconstructions

Bimaterial	ε
PMMA/Titanium	0.087
PMMA/CrCo Alloy	0.090
PMMA/Stainless Steel	0.089
PMMA/UHMWPE	0.047

Results

The material property values used in the analyses are summarised in Table 1, and the bimaterial properties for each possible interface, ϵ, are shown in Table 2. Values for ϵ were calculated using Eq. (1).

For convenience the stress condition at the interface is represented by the ratio σ/τ. Using the material values of Table 2, a plot of crack kinking angle, θ, versus the stress ratio, σ/τ, for different bimaterial interfaces at a crack length of 3 mm has been generated (Fig. 4). The relationship between θ and σ/τ is obtained by rewriting Eqs. (5) in terms of σ/τ and substituting into Eq. (3).

From the literature it is noted that there is considerable variation in the material property values quoted for bone-cement, due, no doubt, to varying manufacturing and preparation techniques. To investigate whether this effects the potential for the crack to leave the interface, crack kinking angle versus Young's Modulus for bone-cement has been plotted, with curves for

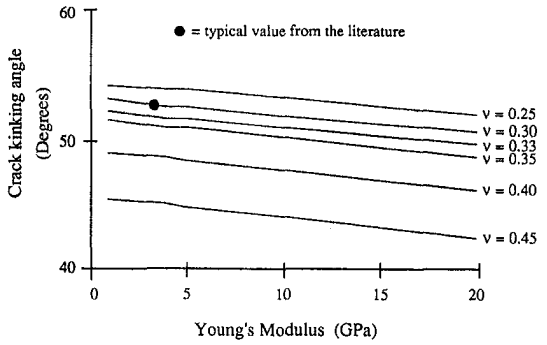

Fig. 5 Young's Modulus of bone-cement versus the crack kinking angle out of the interface for different possible Poisson's ratio, ν, of bone-cement. The interface represented in the figure is that of titanium/bone-cement. Fixed-valued parameters are the titanium properties: ν = 0.33; E = 109 GPa; crack length, a = 3.0 mm; and stress ratio, σ/τ = 2.

different values of Poisson's ratio of bone-cement (Fig. 5). This graph is for a titanium/cement interface where the material properties of the titanium are as shown in Table 1. To demonstrate the trend, results are plotted for a stress ratio, $\sigma/\tau = 2$ and a representative crack length, a, of 3 mm.

Finally, using Eq. (6), mode I stress intensity values, $K_{\theta_{max}}$ were calculated for a titanium/cement interface at a number of initial crack lengths. Figure 6 shows the relationship between $K_{\theta_{max}}$, interface crack length, and stress ratio.

Discussion

The fracture mechanics theory used in this study is for an interface in an idealised infinite plane between two linear elastic materials. The theory is valid for two dimensional, perfectly bonded, smooth interfaces with a sharp crack along the interface. We apply the theory to determine the conditions under which a small crack along a prosthesis/cement interface will enter the cement mantle. The intention is to simulate the initial stages of implant loosening. It is the first step in developing a complete model of the failure process for the complex implant structure, from the perspective of failure by damage accumulation. There are a number of limitations to using linear fracture mechanics to model bimaterial interfaces and these should be considered before discussing the results.

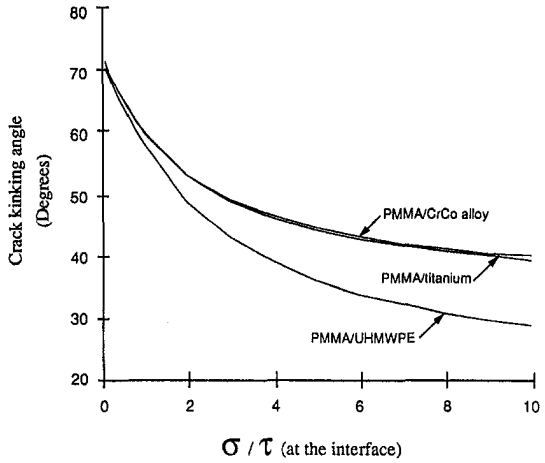

Fig. 4 The ratio of the normal and shear interface stresses, σ/τ, in the vacinity of the crack, versus crack kinking angle, θ. Fixed-valued parameters are the material properties (from Table 1) and the crack dimension, a = 3.0 mm. The curve for PMMA/Stainless Steel is not shown as it lies along the same path as that for PMMA/CrCo alloy.

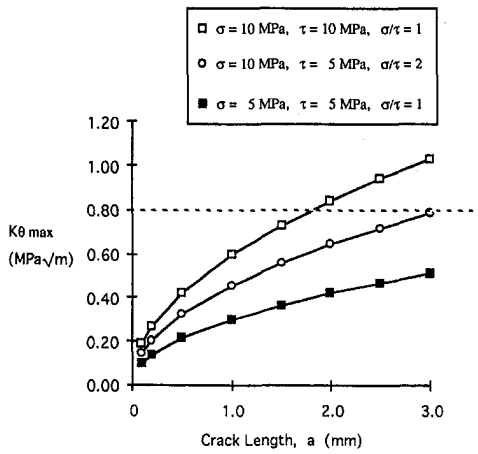

Fig. 6 Critical stress intensity ($K_{\theta_{max}}$) versus interface crack length, a, for different ratios of normal and shear stresses, σ/τ, calculated from Eq. (6) for a titanium/bone-cement interface. The horizontal dashed line is at the lower value of K_{1C} for bone cement reported in the literature (e.g., Rimnac et al., 1986; Robinson et al., 1981).

In reality, implant structures have three dimensional stress states and geometries (Huiskes, 1993). There are many potential sites for crack initiation throughout the structure (Harrigan et al., 1992). Cracks can conceivably grow in any direction and the crack front may have a curved or even jagged profile (Culleton et al., 1993). The bimaterial fracture mechanics theory used in this study is applied only to the local region around one crack in the structure. The analysis is restricted to a crack at the cement/implant interface subjected to in-plane loading, in which case the crack is most likely to propagate in the plane of loading. In addition, the model considers the case of a crack somewhere along the cement/implant interface rather than a crack starting from the proximal or distal edge of the interface. As a first approach to this study of implant interface crack behaviour, such 'within-interface' cracks (Helmke et al., 1992; James et al., 1993) are more easily modelled.

Typically, a crack can be considered small if it is of the order of 1/10th of a major component dimension—such a crack would satisfy the condition of a crack in an "infinite" plane. There is little quantitative information available from the clinical literature on the length of interface cracks, so a crack length of 3 mm was chosen as a representative maximum initial interface crack size based on the observations made by researchers such as Jasty et al. (1991) and others.

The analysis presented here considers only monotonic loading. An implant, on the other hand, undergoes repeated loading and the results of this analysis can not be directly applied to predict lifetime loading conditions. However, it is generally accepted that fracture mechanics analysis for monotonic loading conditions is applicable to fatigue crack growth by taking $\frac{1}{10}$th of the fracture toughness as an approximation to the fatigue threshold. For a more accurate investigation crack growth rates and damage accumulation would need to be investigated using a fracture mechanics model which incorporates cyclic loading conditions. In a previous paper (McCormack and Prendergast, 1996), the authors have discussed the interpretation of the results of the analysis presented here for fatigue loading conditions using a technique acceptable in the fracture analysis of other engineering structures.

At the early stages of the service life it is reasonable to assume that the interface is well bonded. As noted earlier (Helmke et al., 1992; James et al., 1993), flaws do exist along the interface and these can be modelled as the initial crack on an otherwise bonded interface. In the analysis, the bulk of the cement is assumed to be pore free. The consequence of pores distributed throughout the bulk of the cement in the real structure is to reduce the modulii and strength of the cement—the effect of this on the behaviour of the bimaterial interface crack can be assessed using the model presented in this paper. In addition, the strength of the bond will be a function of the surface finish on the implant; this issue is pursued in more detail later in this discussion. Other conditions are also met by the model. For typical values of material properties used in joint replacements the criterion of small ϵ; as specified in Eq. (3) is satisfied. For low monotonic loading conditions and for brittle bone-cement the maximum principal stress criterion for crack propagation direction is a reasonable assumption.

The material properties used in the study are taken from the literature and some of these, in particular interfacial properties, are difficult quantities to extract from experiment. The values selected are used only for the purposes of illustrating the relationship between crack behaviour, under different monotonic loading conditions, and material properties. Experimental verification (McCormack and Prendergast, 1995) of this analysis for specific material, geometry and loading conditions is necessary before endeavouring to develop the theory toward a more complete model of the damage accumulation process of the real structure. What we learn from the analysis is that, in the vicinity of a crack along a prosthesis/cement interface, certain material combinations and certain stress states are more likely to cause the crack to kink into the adjacent cement. It is instructive to address the implications of this local phenomenon in the context of the implant structure as a whole, particularly prior to loss of primary stability.

Knowing what material and stress conditions cause a crack to kink may provide useful information for the implant designer. In the context of service life, a large kink angle means that the crack will be oriented directly into the bulk cement mantle and is likely to continue to propagate in this direction, leading to disintegration of the mantle over a relatively short number of cycles. A more oblique crack angle may not lead to so rapid a disintegration of the implant interlock because the crack will take longer to propagate through the mantle. It might even be deflected back onto the interface under certain stress conditions (Itou, 1988). The results shown in Fig. 4 highlight this point. As the ratio between the normal and shear stresses at the interface (the σ/τ ratio) increases, the angle that the crack kinks into the cement mantle is reduced. Thus, the interface loading critically influences the direction in which an interface crack will kink. An interesting point to note from this result is that the crack kinking angle depends not on the magnitude of the normal and shear interface stresses but on the ratio of these stresses.

As discussed earlier, both normal and shear stresses exist at the crack tip along a bimaterial interface, as illustrated in Fig. 3. Given the three dimensional stress distribution that exists in the real implant structure, it is certain that this situation will arise. If the ratio of these loads is such as to produce a maximum principal stress normal to the interface crack, the crack will want to propagate along the interface according to the maximum principal stress criterion. If the maximum principal stress is aligned along the interface (i.e. pure shear at the crack tip), the crack will tend to branch into one of the adjacent materials. This emphasises the importance of reducing the shear stresses in the region of the interface so as to reduce the crack kinking angle, thus keeping the crack in the vicinity of the interface.

A particular point raised in this study is the influence that cement mechanical properties have on interface crack behaviour. Even under laboratory conditions there are variations in material properties between the different suppliers, due to different ingredients, particle size, use of antibiotic and radiopaque substances (Krause and Mathis, 1988; Linden, 1991; Kindt-Larsen et al., 1995). Under surgical conditions additional variables can be introduced such as mixing technique, method of insertion, pressurisation, cavity preparation (with blood and bony inclusions), pores, and curing temperature. It has been known for some time that these can all lead to variations in the material properties of the in-vivo cement (Saha and Pal, 1984). The predicted crack kinking angle is highly dependent on the bone-cement material properties, as shown in Fig. 5. For example, the lowest stiffness bone-cement, with the lowest Poisson's ratio, will give the greater crack angle. This trend highlights the importance of quality control in the manufacture of bone-cement, and the need to ensure consistency in surgical procedures that do not lower the mechanical properties.

These crack behaviour trends just discussed may be of help in making decisions during the different stages of implant design. In the design of prostheses components, for example the stem section of a hip prosthesis, material selection is of considerable importance—not only because of changes in stem/cement interfacial stress as a result of changes in the Young's modulus (Prendergast et al., 1989), but because the *behavior* of a crack at the interface is altered. The influence of the relative material properties of typical bimaterial interfaces can be seen in Fig. 4. For example, the crack kinking angle, as calculated from the model presented in this paper, is only slightly less for a titanium/cement interface as compared to that for a CrCo alloy/cement interface for any given interface stress ratio. However, the crack angle is considerably less for the polyethylene/cement interface as compared to the metallic prostheses. The

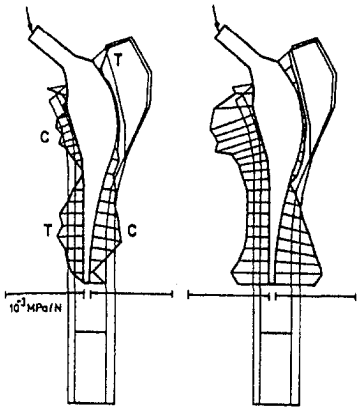

Fig. 7 The stresses generated at the stem/cement interface, where the normal direct stress (tension, compression) is on the left, and the shear stress is on the right (from Huiskes, 1994, by kind permission Hans Huber Publishers)

relevance of Fig. 4 to designers of implants is an awareness of the possible potential crack directions from the coupling of different implant materials, be they at the femoral prosthesis stem, the acetabular cup or at other implant interfaces.

Another example of where the analysis presented here may help to clarify a design decision is the question of which is "best"—rough or polished femoral stems—which has been a controversy for some time (Lee, 1994). Researchers have addressed the issue of stem/cement bonding and debonding using continuum damage mechanics (Verdonschot, 1995) and finite element analysis (Mann et al., 1991). It has been suggested that stem roughness increases the strength (i.e., fracture toughness) of the interfacial bond. In this case, if the interface bond is stronger against crack growth than the adjacent bulk material, a defect existing on the interface would be more likely to propagate out of the interface than along the interface. Polished stems, on the other hand, produce stem/cement interfaces of lower fracture toughness and, although this would seem to be a disadvantage, any crack propagation is likely to be contained along the interface rather than propagating into the cement mantle. This is arguably of clinically benefit in that an interface crack is considered to be less detrimental (i.e., is not usually considered to be a clinical failure) as compared with a disintegrated cement mantle.

Of course, the kinking angles of Figs. 4 and 5 are really *potential* kinking angles. The crack will not grow in these directions unless the stress intensities at the interface crack tip combine to exceed the fracture toughness of either the bulk cement or of the interface. The fracture toughness of the bone cement has been determined experimentally (Rimnac et al., 1986; Robinson et al., 1981) to be in the range 0.8–2.0 MPa.m$^{1/2}$, with similar fracture toughness values being reported for well bonded interfaces (Raab et al., 1981). In this study, using the titanium/cement interface as an example, the stress intensity ahead of the crack tip was calculated as a function of crack length, for different interface stresses (Fig. 6). It is clear from this figure, that the magnitude of normal and shear interface stresses together with the σ/τ ratio and crack length all influence how close the crack tip stress intensity is to the fracture toughness of the cement.

In practice, we know that interface cracks do propagate into the cement, so how do the variables mentioned above combine to initiate crack growth? From studies of the stress patterns obtained using finite element analysis, we can determine the likelihood of an interface defect propagating into the cement mantle. As an example, Fig. 7, from Huiskes (1994), shows the distribution of normal and shear stresses on the cement/implant interface of a hip prosthesis femoral component. For a typical maximum hip joint load of four times body weight (approximately, 3 kN), it can be seen that, for this design of femoral component, the critical region for interface defect propagation into the cement will be distal and medial. The highest predicted normal stress in this region is approximately 1.5 MPa and the shear stress in this region is approximately 1.5 MPa, giving σ/τ of 1.0 and, for a 3 mm interface flaw, a $K_{\theta_{max}}$ of 0.15 MPa.m$^{1/2}$. Harrigan et al. (1992) analyze the cement/femoral stem stress distribution under stair climbing loads. In the areas of highest normal tensile stresses (>3.7 MPa), the shear stress was greater than 1.0 MPa, so the resulting σ/τ ratio is 4, approximately, and $K_{\theta_{max}}$ is 0.27 MPa.m$^{1/2}$ for a 3 mm interface flaw.

In a study of cemented polyethylene acetabular cups, Dalstra (1993) reported cement/implant interface stresses for both metal backed and non-metal-backed components. His results can be used to estimate the potential for cement mantle disintegration from an interface flaw for the different designs. For nonmetal-backed components (UHMWPE/cement interface), the normal and shear stresses are 0.5 MPa and 1.4 MPa, respectively, giving σ/τ of 0.36 and a maximum stress intensity, $K_{\theta_{max}}$ of 0.1 MPa.m$^{1/2}$ for an initial interface crack of 3.0 mm. In comparison, titanium metal-backed components have normal and shear stresses equal to 1.0 MPa and 3.8 MPa respectively giving σ/τ of 0.26 and $K_{\theta_{max}}$ = 0.27 MPa.m$^{1/2}$, for an initial interface crack of 3.0 mm. This suggests that, if crack growth were to occur with the non metal-backed component, the crack would grow into the cement at a slightly shallower angle than for the metal-backed component (Fig. 4). In addition, cracking into the cement mantle is more likely to occur from the metal-backed than from the non metal-backed component.

In conclusion, this initial study of crack propagation paths for an existing interface crack at the implant/cement interface has highlighted a number of points which may be useful for implant designers. First, the ratio of normal to shear interface stress is the controlling variable for crack kinking angle, rather than the absolute value of either stress. Second, different material combinations at an implant interface have fundamentally different crack growth directions. Third, variations in the properties of the bone cement will significantly alter the potential for crack propagation. Finally, using stress data available in the literature, this model predicts that stress intensities close to the fracture toughness in fatigue may indeed occur. This indicates the significance of the cement/implant bond conditions in the fracture process and the need to give attention to this in the component design (McCormack and Prendergast, 1994).

This is an new model for interface crack behaviour in the implant structure. There are many directions in which the approach can be developed including, modelling of cracks at the distal tip or the proximal edge of the prosthesis, consideration of cement/bone interface cracks, and the behavior of existing cracks within the cement mantle itself. These topics are the subject of on-going research by the authors.

References

Clech, J. P., Keer, L. M., and Lewis, J. L., 1985, "A Model of Tension and Compression Cracks with Cohesive Zone at a Bone-Cement Interface," ASME JOURNAL OF BIOMECHANICAL ENGINEERING, Vol. 107, pp. 175–182.

Culleton, T. P., Prendergast, P. J., and Taylor, D., 1993, "Fatigue Failure in the Cement Mantle of an Artificial Hip Joint," *Clinical Materials,* Vol. 12, pp. 95–102.

Dalstra, M., 1993, "Biomechanical Aspects of the Pelvic Bone and Design Criteria for Acetabular Prostheses," Ph.D. thesis, University of Nijmegen, The Netherlands.

Gharpuray, V. M., Dundurs, J., and Keer, L. M., 1991, "A Crack Terminating at a Slipping Interface Between Two Materials," ASME *Journal of Applied Mechanics,* Vol. 58, pp. 960–963.

Harrigan, T. P., Kareh, J. A., O'Connor, D. O., Burke, D. W., and Harris, W. H., 1992, "A Finite Element Study of the Initiation of Failure of Fixation in Cemented Femoral Total Hip Components," *Journal of Orthopaedic Research,* Vol. 10, pp. 134–144.

Harris, W. H., 1994, "Osteolysis and Particle Disease in Hip Replacement, A Review," *Acta Orthopaedica Scandinavica,* Vol. 65, pp. 113–123.

Helmke, H. W., Lednicky, C. L., and Tullos, H. S., 1992, "Porosity of the Cement/Metal Interface Following Cemented Hip Replacement," *Proceedings of the 38th Annual ORS,* p. 364.

Huiskes, R., 1985, "Properties of the Stem-Cement Interface and Artificial Hip Joint Failure," J. L. Lewis and J. O. Galante, eds., *A Workshop on the Bone-Implant Interface,* pp. 86–101, Chicago, AAOS.

Huiskes, R., 1993, "Mechanical Failure in Total Hip Arthroplasty With Cement," *Current Orthopaedics,* Vol. 7, pp. 239–247.

Huiskes, R., 1994, "New Approaches to Cemented Hip-Prosthetic Design," G. H. Buchhorn and H.-G. Willert, eds., *Technical Principles, Design and Safety of Joint Implants,* pp. 227–236, Toronto. Hogrefe and Huber.

Itou, S., 1988, "A Sandwiched Layer Containing an Interface Crack," *Engineering Fracture Mechanics,* Vol. 29(5), pp. 549–555.

James, S. P., Schmalzried, T. P., McGarry, F. J., and Harris, W. H., 1993, "Extensive Porosity at the Cement-Femoral Prosthesis Interface: A Preliminary Study," *Journal of Biomedical Materials Research,* Vol. 27, pp. 71–78.

Jasty, M., Maloney, W. J., Bragdon, C. R., O'Connor, D. O., Haire, T., and Harris, W. H., 1991, "The Initiation of Failure in Cemented Femoral Components of Hip Arthroplasties," *Journal of Bone and Joint Surgery,* Vol. 73-B(4), 551–558.

Kindt-Larsen, T., Smith, D. B., and Jensen, J. S., 1995, "Innovations in Acrylic Bone Cement and Application Equipment," *Journal of Applied Biomaterials,* 6, 75–83.

Krause, W., and Mathis, R. S., 1988, "Fatigue Properties of Acrylic Bone Cements: Review of the Literature," *Journal of Biomedical Materials Research,* 22(A1), 37–53.

Lee, A. J. C., 1994, "Rough or Polished Surface on Femoral Anchorage Stems?", in G. H. Buchhorn and H.-G. Willert, eds., *Technical Principles, Design and Safety of Joint Implants,* pp. 209–211, Toronto. Hogrefe and Huber.

Lewis, J. L., Askew, M. J., Wixson, R. L., Kramer, G. M., and Tarr, R. R., 1984, "The Influence of Prosthetic Stem Stiffness and of a Calcar Collar on Stresses in the Proximal End of the Femur With a Cemented Femoral Component," *Journal of Bone and Joint Surgery,* 66-A(2), 280–286.

Linden, U., 1991, "Mechanical Properties of Bone Cement—Importance of the Mixing Technique," *Clinical Orthopaedics,* 272, 274–278.

Maloney, W. J., Jasty, M., Burke, D. W., O'Connor, D. O., Zalenski, E. B., Bragdon, C., and Harris, W. H., 1989, "Biomechanical and Histological Investigation of Cemented Total Hip Arthroplasties," *Clinical Orthopaedics,* 249, 129–140.

Mann, K. A., Bartel, D. L., Wright, T. M., and Ingraffea, A. R., 1991, "Mechanical Characteristics of the Stem-Cement Interface," *Journal of Orthopaedic Research,* 9, 798–808.

McCormack, B. A. O., and Prendergast, P. J., 1996, "Interface Failure in Implants Cemented With Different Bone-Cements: A Fracture Mechanics Analysis," J. Middleton, M. L. Jones, and G. N. Pande, eds., *2nd International Symposium on Computer Methods in Biomechanics and Biomedical Engineering,* Swansea. Gordon & Breach, Amsterdam, pp. 35–45.

McCormack, B. A. O., and Prendergast, P. J., 1995, "Crack Propagation From Cement/Prosthesis Interface Defects," R. M. Hochmuth, N. A. Langrana, and M. S. Hefzy, eds., *29th ASME Summer Bioengineering Conference,* pp. 275–276, Beaver Creek. ASME.

Prendergast, P. J., Monaghan, J., and Taylor, D., 1989, "Materials Selection in the Artificial Hip Joint Using Finite Element Stress Analysis," *Clinical Materials,* 4, 361–376.

Raab, S., Ahmed, A. M., and Provan, J. W., 1981, "The quasi-static and fatigue performance of the implant/bone-cement interface," *Journal of Biomedical Materials Research,* 15, 159–182.

Rice, J. R., 1988, "Elastic Fracture Mechanics Concepts for Interfacial Cracks," ASME *Journal of Applied Mechanics,* 55, 98–103.

Rice, J. R., and Sih, G. C., 1965, "Plane Problems of Cracks in Dissimilar Media," ASME *Journal of Applied Mechanics,* 32, 418–423.

Rimnac, C. M., Wright, T. M., and McGill, D. L., 1986, "The Effect of Centrifugation on the Fracture Properties of Acrylic Bone Cements," *Journal of Bone and Joint Surgery,* 68-A(2), 281–287.

Robinson, R. P., Wright, T. M., and Burstein, A. H., 1981, "Mechanical Properties of Polymethylmethacrylate Bone Cements," *Journal of Biomedical Materials Research,* 15, 203–208.

Saha, S., and Pal, S., 1984, "Mechanical Properties of Bone Cement: A Review," *Journal of Biomedical Materials Research,* 18, 435–462.

Verdonschot, N., 1995, "Biomechanical Failure Scenarios for Cemented Total Hip Replacements," Ph.D. thesis, University of Nijmegen, The Netherlands.

Verdonschot, N., and Huiskes, R., 1992, "The Application of Continuum Damage Mechanics to Pre-clinical Testing of Cemented Hip Prostheses: the Effects 1575of Cement/Stem Debonding," J. Middleton, G. Pande, and K. Williams, eds., *Recent Advances in Computer Methods in Biomechanics and Biomedical Engineering,* Swansea, pp. 50–57. BJI Ltd.

Yuuki, R., and Xu, J. Q., 1992, "Stress-Based Criterion for an Interface Crack Kinking out of the Interface in Dissimilar Materials," *Engineering Fracture Mechanics,* 41(5), 635–644.